Interfacial shear strength of cured vinyl ester resin-graphite nanoplatelet from molecular dynamics simulations

Changwoon Jang [a,1], Thomas E. Lacy [a], Steven R. Gwaltney [b,*], Hossein Toghiani [c], Charles U. Pittman Jr. [b]

[a] Department of Aerospace Engineering, Mississippi State University, Mississippi State, MS 39762, USA
[b] Department of Chemistry, Mississippi State University, Mississippi State, MS 39762, USA
[c] The David C. Swalm School of Chemical Engineering, Mississippi State University, Mississippi State, MS 39762, USA

ARTICLE INFO

ABSTRACT

Interfacial adhesion between a three layer thick graphite nanoplatelet and a vinyl ester (VE) matrix was studied using molecular dynamics simulations. Polymer interphase formation near carbon surfaces influences interfacial bonding and carbon/matrix load transfer. A VE resin was equilibrated near the graphite surfaces and then cured using the Relative Reactivity Volume algorithm to form a crosslinked matrix while enforcing the correct regiochemistry and relative reactivity ratios within the free radical addition cure. The local styrene monomer concentration in both the liquid and cured resin was highest near the graphite sheets, affecting interfacial strength and near-surface crosslink density. The composite's glass transition temperature (466–502 K) was 50–100 K higher than pure VE. The interfacial shear strength was 141 MPa for resin with 87% monomer conversion and 106 MPa for 98% monomer conversion, indicating effective reinforcement/matrix load transfer. This computational methodology provides more chemically realistic predictions of interfacial surface adhesion than has been reported previously.

1. Introduction

Carbon fibers [1–3] and carbon-based nanofillers, [4–11] including continuous PAN-based and pitch-based fibers, carbon nanotubes (CNTs), carbon nanofibers (CNFs), and graphene sheets have been used in polymeric matrix composites because of their excellent mechanical, electrical, and thermal properties, light weight, tailorability, and multi-functionality. They have been used in aerospace, sports, automotive, and electronic applications [12,13]. In order to maximize carbon-reinforced polymeric properties, matrix-to-carbon adhesion and wetting need to be optimized [14]. The high surface area-to-volume ratios of nanocarbon reinforcements hamper their dispersion in resins because of dramatic increases in resin viscosity [15]. The nanofiller/matrix interfacial shear strength will depend on the properties and structure of any interphase region formed between the reinforcement surface and the bulk resin. When no covalent chemical bonding exists between a reinforcement and polymer matrix, the interfacial shear strength is governed by non-bonded interactions, primarily electrostatic and van der Waals interactions. Some experimental surface measurements [16] indicate mechanical interlocking may also contribute to the interfacial shear strength, but this influence is not considered in this study.

If an interphase/interface region of different structure than the bulk exists, this will create a property gradient between the reinforcement surface and the bulk matrix region. Characterizing interfacial properties between nanoreinforcements and polymer matrices is challenging. Scanning electron microscopy (SEM), transmission electron microscopy (TEM), and atomic force microscopy (AFM) have been used to characterize composite interfacial properties [17–19]. However, SEM can only probe exposed surface areas, and TEM can only examine very small areas with thicknesses of a few nanometers. Such regions may not be representative of the entire material. AFM examination of the interphase region of a thermoset resin requires removal of the bulk region to expose the interphase to the tip. However, the resin is crosslinked to the interphase and this would require breaking many chemical bonds, and doing this without changing the interphase's properties. Such a challenge seems impossible to achieve. Molecular dynamics (MD) simulations have been used to predict some interfacial characteristics. Gou et al. [20] performed MD simulations of a single walled carbon nanotube (SWCNT) pullout from a cured epoxy resin. Li et al. [21] investigated

* Corresponding author. Tel.: +1 662 325 7602.
  E-mail address: drg51@msstate.edu (S.R. Gwaltney).
[1] Present address: Department of Chemical & Biological Engineering, Drexel University, 3101 Ludlow Street, Philadelphia, PA 19104, United States.

the pullout of a SWCNT from a polyethylene (PE) matrix. Liao and Li [22] used MD nanotube pullout simulations to show that the interfacial shear strength for SWCNT/polystyrene (PS) is significantly higher than most conventional carbon fiber reinforced polymer composite systems.

Graphene sheets have remarkable thermal and electrical conductivity and mechanical stiffness [23,24]. Koenig et al. [25] directly measured adhesion energies for monolayer graphene $(0.45 \pm 0.02 \, \mathrm{J \, m^{-2}})$ and multilayer graphene sheets $(0.31 \pm 0.03 \, \mathrm{J \, m^{-2}})$ with a silicon oxide substrate. These large adhesion energies facilitated developments in graphene-based electrical and mechanical devices, where adhesive forces are known to play an important role. Zhao et al. [26] showed a ten-fold enhancement of the Young's modulus and a 150% tensile strength improvement with 1.8 vol% graphene in poly(vinyl alcohol). The present work employs three graphitic layers, and so is not technically graphene, which refers to a single sheet. However, the results presented here should be applicable to true graphene systems, as well as most graphite nanocomposites used currently.

In this work MD simulations were performed using Accelrys Materials Studio v5.0 [27] and the Condensed-phase Optimized Molecular Potentials for Atomistic Simulation Studies (COMPASS) force field [28] to investigate polymer properties in the vicinity of a carbon surface. A three layer thick graphite nanoplatelet (in-plane dimensions $32 \times 32 \, \text{Å}^2$) was used to serve as a sample pristine carbon surface to mimic the interaction of unoxidized carbon reinforcements with a cured vinyl ester (VE) resin. The total repeating unit cell (RUC) size was $32 \times 32 \times 60 \, \text{Å}^3$. The interfacial shear strength determined here was calculated using a procedure that is applicable to all resin/solid material interfaces. First, the monomer mixture used to generate the final cured resin was equilibrated to generate the liquid monomer distribution gradient that would be established in the surface region. Then, this liquid monomer was cured using our recently developed Relative Reactivity Volume (RRV) curing algorithm [29], which is more chemically realistic than other prevalent approaches [20–22]. This method incorporates the proper head-to-tail regioselectivity and the known monomer relative reactivity ratios (hence, realistic monomer sequence distributions in the cured resin) into the curing process. Regular relaxations of the entire RUC contents during curing were performed. Thus, effects of the surface on monomer diffusion and orientation and conformational effects of the developing crosslinked resin are partially captured. The procedure followed here allows for the development of a liquid monomer interphase zone of different monomer composition than is present in the bulk liquid resin. The curing begins using this spatially varying equilibrated monomer composition and applies regioselectivity and relative reactivity ratios, while permitting monomer and polymer diffusion to occur intermittently during the cure. This allows the graphite surfaces to continue to influence the crosslink network formation. The final result is a cured resin composition, where a thin interphase region at, and extending away from, the graphite surfaces exist. This region has a monomer composition different than that of the bulk matrix. Since certain monomers are enriched in the cured resin composition at the surface, the interfacial shear strength differs from that which would occur if the matrix structure at the graphite surface was the same as the bulk matrix structure.

2. Simulation method details

Commercial Derakane 441-400 VE resin (Ashland Co.) was modeled in this study. It contains 33 wt% of the co-monomer styrene as a diluent to lower VE resin viscosity. Derakane 441-400 has an average of 1.62 bisphenol-A groups per monomer ($n = 1.62$) [30] in the dimethacrylate backbone as shown in Fig. 1. A VE resin model

was created for $n = 1$ and 2 in the appropriate ratio to create an average $n = 1.62$. For simplicity, these two dimethacrylate monomers are designated VE1 and VE2, corresponding to $n = 1$ and 2, respectively, in Fig. 1.
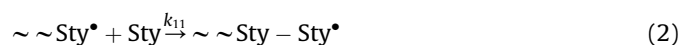
All MD simulations were carried out using Accelrys Materials Studio v5.0 [27] with the COMPASS force field [28]. A three dimensional (3D) periodic simulation cell size of $32 \times 32 \times 60 \, \text{Å}^3$ was created. Three centrally located graphite sheets were positioned parallel to the xy plane and were separated by 3.5 Å in the middle of the box. Three graphite sheets were chosen so that the resin monomers on either side of the sheets would be farther away than the 9.5 Å cutoff used for the van der Waals interactions. Electrostatic interactions between monomers on opposite sides of the graphite sheets are still included, but these are expected to be small. Vinyl ester (VE) resin monomers (styrene, VE1, and VE2) were randomly packed around both sides of the graphite sheets to fill the cell, yielding a final simulation cell density of 1.20 g/cm^3. The monomers occupied the volume on both sides of the three sheet graphite stack to a distance of 26 Å from both sides of the sheet surfaces.

The energy of the system was initially minimized for 10,000 iterations. Then the system was heated from 10 K to 1000 K in 50 K increments within the NVT ensemble. Dynamics simulations were run for 10 ps with a 1 fs time step (a total of 10,000 iterations) at all intermediate temperatures. At 1000 K dynamics simulations were run for 7 ns with a 1 fs time step to achieve equilibration. Once the system equilibration was achieved at 1000 K, the system was cooled to room temperature (300 K) in 50 K decrements using the same procedure as during the heating phase. After cooling the system was re-equilibrated at 300 K through 3 ns of dynamics simulation.

After monomer equilibration a crosslinked network was created using the RRV method [29]. The RRV method incorporates three critical features of any resin's curing. (1) First, regioselectivity (head-to-tail chain propagation) is enforced. (2) Second, the relative reactivity ratios (r_1 and r_2) during polymerization of different monomers are accounted for. (3) Third, imposing the relative reactivity ratios allows for monomer concentration drift and the formation of the correct monomer sequence distributions during curing. Since the VE resin contains both styrene and dimethacrylate monomers (VE1 and VE2), different polymerizable functional groups exist. The terminal polymerization model was used, where the assumption is made that the reactivity of a growing chain depends only on the reactivity of the end (terminal) monomer of the chain and not on any other monomer within that chain or on the chain length [31,32]. The terminal copolymerization model is expressed as

$$\frac{dM_1}{dM_2} = \frac{M_1(r_1 M_1 + M_2)}{M_2(r_2 M_2 + M_1)} \tag{1}$$

where M_1 and M_2 represent the concentration of styrene molecules and VE dimethacrylate molecules for a styrene-containing VE resin, respectively [31,32]. The reactivities of VE1 and VE2 were treated as equivalent since they have identical polymerizing methacrylate functional groups. The relative reactivity ratios, r_1 and r_2, are defined by the rate constants ratios ($r_1 = k_{11}/k_{12}$ and $r_2 = k_{22}/k_{21}$). The rate constants (k_{11}, k_{12}, k_{22}, k_{21}) are for the chain growth steps shown in Equations 2–5.

$$\sim\sim \text{Sty}^{\bullet} + \text{Sty} \overset{k_{11}}{\rightarrow} \sim\sim \text{Sty} - \text{Sty}^{\bullet} \tag{2}$$

$$\sim\sim \text{Sty}^{\bullet} + \text{VE} \overset{k_{12}}{\rightarrow} \sim\sim \text{Sty} - \text{VE}^{\bullet} \tag{3}$$

$$\sim\sim \text{VE}^{\bullet} + \text{VE} \overset{k_{22}}{\rightarrow} \sim\sim \text{VE} - \text{VE}^{\bullet} \tag{4}$$

$$\sim\sim \text{VE}^{\bullet} + \text{Sty} \overset{k_{21}}{\rightarrow} \sim\sim \text{VE} - \text{Sty}^{\bullet} \tag{5}$$